Effect of Thermal Radiation on Non-Darcy Hydromagnetic Convective Heat and Mass Transfer Flow of a Water-SWCNT's Nanofluid in a Cylindrical Annulus with Thermo-Diffusion and Chemical Reaction

Dr. P.Vijayalakshmi
Associate Professor in Mathematics,
Gates Institute of Technology,Anantapuramu-515001,A.P,India

Abstract : An analysis has been made to investigate the flow of Water-Swcnt's nanofluid in a concentric annular region in the presence of non-uniform heat sources. The non-linear equations have been solved by employing Galerkine finite element method with quadratic polynomials. The velocity, temperature and nano-concentration have been analysed for different parametric values .It is noticed that higher the radiative heat flux(Rd)/nanoparticle volume fraction(ϕ) larger the temperature and concentration while smaller the velocity with ϕ,larger with Rd. Higher thermo-diffusion smaller the concentration and larger with chemical reaction effects.

Keywords : Circular annulus, Swcnt's-nanofluid, thermal Radiation, Soret effect, chemical reaction, Non-Uniform heat sources

1. INTRODUCTION:

Originally discovered in 1995,nanofluids are a class of fluids that have been attracted significant attention of researchers in various fields. Owing to their advantages, nanofluids have been implemented in various industrial sectors, such as energy and biomedical fields. Choi (9) reported that the thermal conductivity of nanofluids can be enhanced by dispersing nanosized particles in the fluid. Moreover, it was discovered that the flow of the base fluid improved by suspended nanoparticles in it(29a). During the past decade the technology of producing particles in nanometer dimensions was improved and a new kind of solid-liquid mixture that is called nanofluid was established by Choi [9]. The dispersion of a small amount of solid nanoparticle in conventional fluids such as water or Ethylene glycol changes their thermal conductivity remarkably. In general, in most recent research areas, heat transfer enhancement in forced convection is desirable [Behzadmchr et al[6], Bianco et al [7] and Santro [43]], but there is still a debate on the effect of nano-particles on heat transfer enhancement in natural convection applications. Natural convection of Al_2O_3-water and CuO-water nanofluid inside a cylindrical enclosure heat from one side and cooled from the other side was studied by Putra et al., [31]. They found that the natural convection heat transfer coefficient was lower than that of pure water. Wen and Ding [44] investigated the natural convection of TiO_2-water in a vessel composed of two discs. Their results showed that the natural convection decreases by increasing the volume fraction of nanoparticle. Jou and Tzeng [16] conducted a numerical study of natural convection heat transfer in rectangular enclosure filled with the stream function-vorticity formulation. They investigated the effects of Rayleigh number, the aspect ratio of the enclosure, and the volume fraction of the nanoparticle on the heat transfer inside the enclosures. Their results showed that the average heat transfer coefficient increased with increasing the volume fraction of the nanoparticle. Mokhtari Moghari et al. [25] quested two phase mixed convection Al_2O_3-water nanofluid flow in an annulus. Thermal conductivity variation on natural convection flow of water-alumina nanofluid in annulus is investigated by Parvin et al. [30]. Soleimani et al. [37] studied natural convection heat transfer in a nanofluid filled semi-annulus enclosure. Abu-Nada et al. [1] studied natural convection heat transfer enhancement in horizontal concentric annuli using nanofluid. Abu-Nada [2] investigated the effect of variable viscosity and thermal conductivity of Al_2O_3-water nanofluid on heat transfer enhancement in natural convection. Das et al [11] have studied mixed convective magneto hydrodynamic flow in a vertical channel filled with nanofluids. Sreedevi et al. [38] has investigated mixed convective heat and mass transfer flow of nanofluids in concentric annulus with constant heat flux. Sudarsana et al., [39] have analyzed the Soret and Dufour effects on MHD convective flow of Al_2O_3-water and TiO2-water nanofluids past a stretching sheet in porous media with heat generation with heat generation/absorption. Madhusudhana Reddy et al., [22] have presented Numerical study of Convective Flow of CuO-water and Al_2O_3-water Nanofluids in

cylindrical annulus. Sulochana et al [40] have discussed heat and mass transfer flow in cylindrical annulus in presence of heat sources.

Meanwhile ,the carbon nanotubes (CNT's) have become one of the most effective materials, owing to their ability to enhance the thermal characteristics of the fluid, high electrical conductivity, unique optical transmission, and high tensile strength. They can also increase the entropy generation Berrehal [7]. Shafiq et al [35] CNT'S are rolled–up grapheme sheets arranged in a cylindrical shape. They are of two types single walled (SWCNT's)) and multi-walled (MWCNT's). It was observed that the boundary layer separation could be delayed if suction effects on the CNT's nanoparticle volume fraction are provided Annar [4]. According to Naganthran et al [26] and Ahmad et al [3], CNT's have higher thermal conductivity .When dispersed in the based fluid, they can accelerates the rate of the heart transfer and subsequently increase the base fluid 's thermal conductivity. Using Buongiorno's concept, Khan et al [19] analysed the effects of Brownian motion and thermophoresis on the CNT's flow using Xue's model. Annur et al [5] reported the enhanced performance of CNT's owing to the existence of the velocity slip in boundary conditions. Kamali and Binesh [17] numerically investigated the convective heat transfer of multi-wall carbon nano-tube (MWCNT)-based nanofluids in a straight tube under constant wall heat flux condition. They solved Navier-Stokes equations using the finite volume technique considering CNT-based nanofluids using power law model. They found that the heat transfer coefficient is dominated by the wall region due to non-Newtonian behaviour of CNT nanofluid. Meyer et al [24] investigated experimentally the convective heat transfer enhancement of aqueous suspension of multi-walled CNT's flowing through a straight horizontal tube. They determined the heat transfer coefficient and friction factor as a function of Reynolds number. Wang et al [43] experimentally investigated the heat transfer and pressure drop of nanofluids containing CNT's in a horizontal circular tube. Kumaresan et al [20] reported an experimental study on the convective heat transfer characteristics of a secondary refrigerant-bases CNT nanofluids in tubular heat exchanger. Ebaid and Sharif [12] suspended CNT's in a base fluid and studied the effect of a magnetic field on fluid motion and enhanced the rate of heat transfer of nanofluids using CNT's. Hong et al [15] have been discussed to enhanced thermal conductivity by the magnetic field in heat transfer nanofluids containing carbon nanotube.

Thermal motion of the charged particles produces electromagnetic radiation called thermal radiation. Every matter emits thermal radiation at a temperature greater than absolute zero (absolute temperature is also called thermodynamic temperature). When the absolute temperature is less than the body temperature, kinetic energy of molecules change due to inter-atomic collisions. Heat transfer in the presence of thermal radiation has many applications in physics, industrial engineering, space technology for example gas cooled nuclear reactors, aerodynamics rockets, large open water reservoirs, thermal power engineering and so forth. Rosseland approximation has been considered by numerous researchers for radiation effect. This type of approximation comprises dimensionless variables called radiation parameter and Prandtl number which are supportable for linearized Rosseland approximation if the temperature difference between the plate and ambient liquid is small. Radiative flow over a stretched surface is examined by Cortell. [10]. Sheikholeslami et al. [36] investigated MHD two phase nano-liquid flow with thermal radiation. Reddy et al. [33] examined the impact of nonlinear radiation in three-dimensional MHD flow of ferromagnetic liquid subject to temperature dependent viscosity. Natural convection along a vertical isothermal plate with linear and nonlinear thermal radiations is studied by Pantokratoras [29]. Consequences of nonlinear thermal radiation and heterogeneous-homogeneous reactions in flow based on $Ag–H_2O$ and $Cu–H_2O$ nano-material by a stretched cylinder is presented by Qayyum et al. [32]. Nonlinear radiative flow with temperature dependent viscosity in thin liquid film towards a stretched surface is examined by Pal and Saha [28]. Significance of nonlinear radiation in mixed convection flow of magneto Walter-B nano-liquid is explored by Khan et al. [18]. Mixed convective flow with nonlinear thermal radiation of Oldroyd-B liquid near a stagnation region is studied by Hayat et al. [14]. MHD nano-liquid slip flow with entropy generation and nonlinear thermal radiation in a porous vertical micro-channel is considered by López et al. [21]. Simultaneous effect of gyrotactic microorganisms and nonlinear thermal radiation on Magneto-Burgers nano-material is scrutinized by Khan et al. [18]. Xue [45] was studied to model for thermal conductivity of carbon nanotube-based composites.

The objective of this study is to investigate and highlight the effect of thermal radiation and heat source effect on convective heat transfer flow of SwCNt's in the case of concentric annulus. This is performed by employing a theoretical mathematical model, previously introduced by Tiwari and Das [42]. Their model presented the effect of nanoparticles volume fraction in influencing the viscosity of nanofluid.

The behaviour of velocity, temperature and concentration is analyzed at different axial positions. The shear stress and the rate of heat and mass transfer have also been obtained for variations in the governing parameters.

2. FORMULATION OF THE PROBLEM:

We analyse the mixed convective flow of a SWCNt-water nanofluid in a vertical circular annulus through a porous medium whose walls are maintained at a constant heat flux and uniform concentration. The flow, temperature and concentration in the fluid are assumed to be fully developed. Both the fluid and porous region have constant physical properties and the flow is a mixed convection flow taking place under thermal and molecular buoyancies and uniform axial pressure gradient. The Boussinesque approximation is invoked so that the density variation is confined to the thermal and molecular buoyancy forces. The Brinkman-Forchhimer-Extended Darcy model which accounts for the inertia and boundary effects has been used for the momentum equation in the porous region. The momentum, energy and diffusion equations are coupled and non-linear. Also the flow is unidirectional along the axial direction of the cylindrical annulus. Making use of the above assumptions the governing equations are

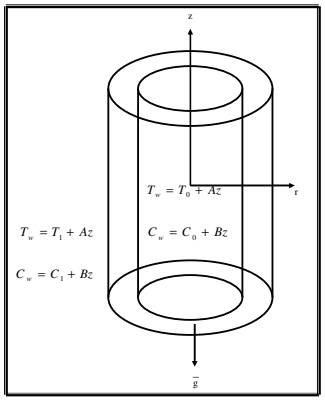

Fig.1 : CONFIGURATION OF THE PROBLEM

$$-\frac{\partial p}{\partial z}+\frac{\mu_{nf}}{\rho_{nf}\delta}\left(\frac{\partial^2 u}{\partial r^2}+\frac{1}{r}\frac{\partial u}{\partial r}\right)-(\frac{\mu_{nf}}{\rho_{nf}k})u-\frac{\sigma_{nf}\mu_e^2 H_0^2}{\rho_{nf}r^2}-\frac{\delta F}{\rho_{nf}\sqrt{k}}u^2+(\rho\beta)_{nf}(T-T_i)=0 \quad (2.1)$$

$$(\rho C_p)_{nf}\,u\frac{\partial T}{\partial z}=k_{nf}(\frac{\partial^2 T}{\partial r^2}+\frac{1}{r}\frac{\partial T}{\partial r})+q'''-\frac{1}{r}\frac{\partial (rq_r)}{\partial r} \quad (2.2)$$

$$u\frac{\partial C}{\partial z}=D_B\left(\frac{\partial^2 C}{\partial r^2}+\frac{1}{r}\frac{\partial C}{\partial r}\right)-k_c^{'}C+\frac{D_m K_T}{T_s}\left(\frac{\partial^2 T}{\partial r^2}+\frac{1}{r}\frac{\partial T}{\partial r}\right) \quad (2.3)$$

where u is the axial velocity in the porous region, T , C are the temperature and concentration of the fluid, k is the permeability of porous medium, k_f is the thermal diffusivity, F is a function that depends on Reynolds number, the microstructure of the porous medium and D_B is the molecular diffusivity, D_m is the mass diffusivity, K_T mass diffusion ratio, β is the coefficient of the thermal expansion, q_R is the radiation absorption coefficient, Cp is the specific heat, ρ is density ,g is gravity, ρ_{nf} is the effective density . μ_{nf} is the effective dynamic viscosity, k_{nf} is the thermal conductivity of the nanofluid.

The relevant boundary conditions are

$u=0$, T=T_w , C=C_w at r = a&a+s (2.4)

Following Tao [41], we assume that the temperature and concentration of the both walls is $T_w = T_0 + Az$, $C_w = C_0 + Bz$ where A and B are the vertical temperature and concentration gradients which are positive for buoyancy –aided flow and negative for buoyancy –opposed flow, respectively, T_0 and C_0 are the upstream reference wall temperature and concentration ,respectively.

The coefficient q''' is the rate of internal heat generation (>0) or absorption(<0). The internal heat generation /absorption q''' is modeled as (Emad and Abo-Eldahab et al[13]) as

$$q''' = (\frac{k_f}{a^2 \nu})(A^{\bullet}(T_w - T_0)u + B^{\bullet}(T - T_0)) \quad (2.5)$$

Where $A^{\bullet}$ and $B^{\bullet}$ are coefficients of space dependent and temperature dependent internal heat generation or absorption respectively. It is noted that the case $A^{\bullet}$>0 and $B^{\bullet}$>0, corresponds to internal heat generation and that $A^{\bullet}$<0 and $B^{\bullet}$<0, the case corresponds to internal heat absorption case.

We now define the following non-dimensional variables for the fully developed laminar flow in the presences of radial magnetic field, the velocity depend only on the radial coordinate and all the other physical variables except temperature, concentration and pressure are functions of r and z, z being the vertical co-ordinate .The temperature and concentration inside the fluid can be written as

$T = T^{\bullet}(r) + Az$, $C = C^{\bullet}(r) + Bz$ (2.6)

The effective density of the nanofluid is given by

$\rho_{nf} = (1-\varphi)\rho_f + \varphi\rho_s$ (2.7)

Where ϕ is the solid volume fraction of nanoparticles. Thermal diffusivity of the nanofluid is

$$\alpha_{nf} = \frac{k_{nf}}{(\rho C_p)_{nf}} \tag{2.8}$$

Where the heat capacitance C_p of the nanofluid is obtained as

$$(\rho C_p)_{nf} = (1-\varphi)(\rho C_p)_f + \varphi(\rho C_p)_s \tag{2.9}$$

And the thermal conductivity of the nanofluid k_{nf} for spherical nanoparticles can be written as

$$\frac{k_{nf}}{k_f} = \frac{(k_s + 2k_f) - 2\phi(k_f - k_s)}{(k_s + 2k_f) + \phi(k_f - k_s)} \tag{2.10}$$

The thermal expansion coefficient of nanofluid can determine by

$$(\rho\beta)_{nf} = (1-\varphi)(\rho\beta)_f + \varphi(\rho\beta)_s \tag{2.11}$$

Also the effective dynamic viscosity of the nanofluid given by

$$\mu_{nf} = \frac{\mu_f}{(1-\varphi)^{2.5}}, \tag{2.12}$$

$$\sigma_{nf} = \sigma_f\left(1 + \frac{3(\sigma-1)\phi}{\sigma + 2 - (\sigma-1)\phi}\right), \sigma = \frac{\sigma_s}{\sigma_f}$$

Where the subscripts nf, f and s represent the thermo physical properties of the nanofluid, base fluid and the nanosolid particles respectively and ϕ is the solid volume fraction of the nanoparticles. The thermo physical properties of the nanofluid are given in Table 1.

The thermo physical properties of the nanofluids are given in Table 1 (See Oztop and Abu-Nada [27]).

Table – 1

Physical properties	Fluid phase (Water)	**Swcnt's**	**Mwcnt's**
C_p(j/kg K)	4179	**425**	**796**
ρ(kg m^3)	997.1	**2600**	**1600**
k(W/m K)	0.613	**6600**	**3000**
βx10^{-5} 1/k)	21	2.0	**2.0**
σ	**0.05**	**10^6**	**10^7**

We now define the following non-dimensional variables

$$z^* = \frac{z}{a} \quad , \quad r^* = \frac{r}{a} \quad , \quad u^* = (\frac{a}{\nu})u \ , \ p^* = \frac{pa\delta}{\rho\nu^2} \ ,$$

$$\theta^*(r^\bullet) = \frac{T^\bullet - T_0}{P_1 Aa} \quad , \quad C^*(r^\bullet) = \frac{C^\bullet - C_0}{P_1 Ba} \ , \ s^* = \frac{s}{a}, P_1 = \frac{dp}{dx} \tag{2.13}$$

Introducing these non-dimensional variables, the governing equations in the non-dimensional form are (on removing the stars)

$$(\frac{\partial^2 u}{\partial r^2} + \frac{1}{r}\frac{\partial u}{\partial r}) = A_1 A_3 + \delta A_1 (D^{-1} + \frac{A_6 M^2}{r^2})u + \delta^2 A_1 (D^{-1})^{1/2}\Delta u^2 - \delta A_1 A_4 G(\theta) \tag{2.14}$$

$$A_2(1 + \frac{4Rd}{3})(\frac{\partial^2\theta}{\partial r^2} + \frac{1}{r}\frac{\partial\theta}{\partial r}) + (A1u + B1\theta) = A_5 \Pr u \tag{2.15}$$

$$(\frac{\partial^2 C}{\partial r^2} + \frac{1}{r}\frac{\partial C}{\partial r}) - \gamma C = Sc\,u + ScSr\left(\frac{\partial^2\theta}{\partial r^2} + \frac{1}{r}\frac{\partial\theta}{\partial r}\right) \tag{2.16}$$

Where

$\Delta = FD^{-1/2}$ (Inertia parameter or Forchheimer number), $G = \frac{g\beta(T_e - T_i)a^3}{\nu^2}$ (Grashof number),

$M^2 = \frac{\sigma\mu_e^2 H_0^2}{a\nu}$ (magnetic parameter), $D^{-1} = \frac{a^2}{k}$ (Inverse Darcy parameter),

$P_r = \frac{\mu C_p}{k_f}$ (Prandtl number), $Sc = \frac{\nu}{D_B}$ (Schmidt number) , $\gamma = \frac{k_c^1 a^2}{D_B}$ (Chemical Reaction parameter),

$So = \frac{D_m K_T (T_0 - T_{i)}}{T_s (C_0 - C_i)}$ (Soret parameter)

$A_1 = \frac{1}{(1-\varphi)^{2.5}}$, $A_2 = (1-\varphi) + \varphi(\frac{\rho_s}{\rho_f})$, $A_3 = 1 - \varphi + \varphi \frac{(\rho C_p)_s}{(\rho C_p)_f}$, $A_4 = 1 - \varphi + \varphi(\frac{(\rho\beta)_s}{(\rho\beta)_f}$,

$A_5 = \frac{k_{nf}}{k_f}$ $A_6 = (1 + \frac{3(\sigma - 1)}{\sigma + 2 - (\sigma - 1)\phi})$, $\sigma_{nf} = \sigma_f A_6$, $\sigma = \frac{\sigma_s}{\sigma_f}$

The corresponding non-dimensional conditions are

$u = 0 \quad \theta = 0$ C=0 at r=1 and 1+s (2.17)

3. FINITE ELEMENT ANALYSIS

The finite element analysis with quadratic polynomial approximation functions is carried out along the radial distance across the circular duct. The behavior of the velocity, temperature and concentration profiles has been discussed computationally for different variations in governing parameters. The Galerkin method has been adopted in the variational formulation in each element to obtain the global coupled matrices for the velocity, temperature and concentration in course of the finite element analysis.

Choose an arbitrary element e_k and let u^k, θ^k and C^k be the values of u, θ and C in the element e_k. We define the error residuals as

$$E_p^k = \frac{d}{dr}\left(r\frac{du^k}{dr}\right) + \delta A_1 A_4 G(\theta^k) - \delta A_1 (D^{-1} + \frac{A_6 M^2}{r^2}) r u^k - A_1 \delta^2 \Delta r (u^k)^2 - A_1 A_3 \qquad (3.1)$$

$$E^k{}_\theta = \frac{A_2}{\Pr}\frac{d}{dr}\left(r\frac{d\theta^k}{dr}\right) - A_5 r u^k + (A_{11} u^k + B_{11}\theta^k) \qquad (3.2)$$

$$E^k{}_c = \frac{d}{dr}\left(r\frac{dC^k}{dr}\right) - rScu^k - \gamma C^k + ScS_r \frac{d}{dr}\left(r\frac{d\theta^k}{dr}\right) \qquad (3.3)$$

where u^k, θ^k & C^k are values of u, θ& C in the arbitrary element e_k. These are expressed as linear combinations in terms of respective local nodal values.

$$u^k = u_1^k \psi_1^k + u_2^k \psi_1^k + u_3^k \psi_3^k$$
$$\theta^k = \theta_1^k \psi_1^k + \theta_2^k \psi_2^k + \theta_3^k \psi_3^k$$
$$C^k = C_1^k \psi_1^k + C_2^k \psi_2^k + C_3^k \psi_3^k$$

where ψ_1^k, ψ_2^k --------- etc are Lagrange's quadratic polynomials.

Galarkin's method is used to convert the partial differential Equations (3.1) – (3.3) into matrix form of equations which results into 3x3 local stiffness matrices. All these local matrices are assembled in a global matrix by substituting the global nodal values and using inter element continuity and equilibrium conditions. The resulting global matrices have solved by iterative procedure until the convergence i.e $|u_{i+1}-u_i| < 10^{-6}$ is obtained.

4. SHEAR STRESS,NUSSELT NUMBER AND SHERWOOD NUMBER

The shear stress (τ) is evaluated using the formula $\tau = (\frac{du}{dr})_{r=1,1+s}$. The rate of heat transfer (Nusselt number) is evaluated using the formula $Nu = -(\frac{d\theta}{dr})_{r=1,1+s}$. The rate of mass transfer (Sherwood number) is evaluated using the formula $Sh = -(\frac{dC}{dr})_{r=1,1+s}$

5. COMPARISON

In the absence of magnetic field (M=0), Thermal radiation (Rd=0), Soret parameter (So=0) the results are in good agreement with Sulochana et al[40].

Table – 2

Parameter		Sulochana et al [40]		**Present Results**		Sulochana et al [40]		**Present Results**	
		Cuo-water		**Cuo-water**		Al_2O_3		**Al_2O_3**	
		τ(1)	τ(2)	**τ(1)**	**τ(2)**	Nu(1)	Nu(2)	**Nu(1)**	**Nu(2)**
ϕ	**0.05**	-0.344709	0.295543	**-0.344712**	**0.295541**	-0.375427	0.309548	**-0.375426**	**0.309549**
	0.1	-0.322286	0.234133	**-0.322288**	**0.234129**	-0.356835	0.243367	**-0.356834**	**0.243369**
	0.3	-0.298190	0.199080	**-0.298192**	**0.199075**	-0.305607	0.155813	**-0.305601**	**0.155816**
	0.5	-0.166095	0.166046	**-0.166089**	**0.166042**	-0.204787	0.125445	**-0.204782**	**0.125449**
Δ	**2**	-0.344709	0.295543	**-0.344702**	**0.295539**	-0.375427	0.309548	**-0.375424**	**0.309551**
	4	-0.835576	0.757665	**-0.835569**	**0.757659**	-0.904463	0.866134	**-0.904459**	**0.866136**
	6	-1.793485	1.213450	**-1.793481**	**1.213452**	-1.855349	1.234368	**-1.855342**	**1.234366**
	10	-2.329867	2.148234	**-2.329862**	**2.148236**	-2.454894	2.357145	**-2.454896**	**2.357142**

6. RESULTS AND DISCUSSION

The non-linear governing equations of the flow, heat and mass transfer have been solved by employing Galerkine finite element analysis with quadratic approximation polynomials. We have chosen here Pr=6.2 while M, A11,B11, Sc, Rd, γ, Q1, Ec, ϕ are varied over a range, which are listed in the Figure legends.

Fig.2a represents the effect of magnetic parameter M on the nanofluid velocity profile. It is observed from the figure that the velocity distribution decreases with increasing magnetic parameter M. This depreciation can be attributed to the fact that the magnetic field provides a resistive type of force known as the Lorentz force. This force tends to lessen the motion of the fluid for higher values of M. as a consequence the velocity reduces. This phenomenon has good agreement with the physical realities. Fig.2b represents the effect of magnetic parameter M on the nanofluid temperature profile. It is observed from the profiles that the temperature distribution increases with increasing values of M, as a result of growth in the thickness of the thermal boundary layer owing to the Lorentz force developed by the magnetic field. This phenomenon has good agreement with the physical realities The effect of magnetic field (M) on the nanoconcentration (C) shows that increasing M leads to a growth in the thickness of the solutal boundary layer which results in the enhancement of the nanoconcentration in the flow region. This phenomenon has good agreement with the physical realities.

Figs.3&4 depicts the behaviour of the velocity with heat source parameters A11&B11. It is found that axial velocity increases with increase in the strength of the space dependent heat source / sink. This is due to the fact that when heat is generated, the buoyancy forces increases which enhances the flow rate and there by gives rise to an enhancement in the velocity profile .An increase in the heat generating heat source (fig.4a) decreases the axial velocity and in the presence of heat absorbing source the velocity increases in the entire flow region.Figs.3b&4b depicts the behaviour of the temperature with space dependent/temperature dependent heat source parameter (A11,B11). It is found that temperature exhibits an increasing tendency with increase in the strength of the heat generating source and reduces with space dependent (fig.4b). This is due to the fact that the presence of the heat generating source generates energy in the thermal boundary layer and as a consequence the temperature rises in the annular region. In the case of space dependent heat sink/absorption source (A11<0,B11<0) (fig.3&4b) the temperature reduces with decreasing values of B11<0, owing to the absorption of energy in the thermal in the flow region. This may be due to the fact that heat is absorbed in the boundary layer in the presence of temperature dependent absorbing source.Fig.5c&6c represent the nanoparticle concentration (C) with A11&B11.An increase in the strength of the space dependent heat source leads to an enhancement in the nanoconcentration in the nanofluid while a reversed is true in the case of heat sink(fig.3c). From fig.5c the nanoconcentration reduces with B11>0 and enhances with B11<0.

Fig.5c shows the variation of C with Schmidt number(Sc).From the profiles we find that the concentration experience a depreciation with increasing Sc.

Figs.6c represents the concentration (C) with chemical reaction parameter γ.It can be seen from the concentration profiles that the concentration enhances in both the degenerating /generating chemical reaction cases.

Figs.7a-7c show the variation of radiation absorption(Q1) on u,θ and C. From the figures we find that higher the radiation absorption(Q1) smaller the velocity, nanoconcentration and larger the temperature in the flow region. This may be due to the fact that increase in Q1 leads to a decay in thickness of momentum and solutal boundary layers and growth in thickness of the thermal boundary layer.

Fig.8a represents the nanofluid velocity with thermal radiation parameter(Rd).It can be seen from the profiles that higher the thermal radiative heat flux larger the velocity in Swcnt nanofluid.Fig.8b shows the

variation of temperature with Rd. From the profiles we notice that the temperature distribution enhances with increasing Rd in the flow region. This may be due to the growth of the thickness of the thermal boundary layer.Fig.8c shows the variation on nanoconcentration (C) with Rd. From the profiles we find that higher the radiative heat flux smaller the concentration in the solutal boundary layer in SWCNT's nanofluid.

Fig.9a represents the variation of velocity with Eckert number(Ec).From the profiles we find that higher the dissipative force smaller the velocity. This is due to the fat that increase in Ec decays the thickness of the momentum boundary layer.Fig.9b depicts the effect of Ec on θ.It can be see from the profiles that higher the dissipative energy larger the thickness of the thermal boundary which leads to a rise in temperature in the flow region.Fiug.9c show the variation of concentration with Ec. A rise in Ec decays the thickness of the solutal boundary layer which leads to a fall in nanoconcentration in the flow region.

The variation of velocity with Forchheimer parameter (Δ) is exhibited in Fig.10a. It is found that velocity shows a depreciation with increasing the values of Δ in the flow region. This is due to the fact that the thickness of the boundary layer decays with higher values of Δ in SWCNT-water nanofluid. Fig.10b shows the variation of temperature with Δ. It is found that an increase in Δ reduces the temperature in the thermal boundary layer. Fig.10c depicts the concentration with Δ.It can be seen from the profiles that the concentration depreciates with increase in Δ. Thus in the presence of non-darcy flow the velocity, nanoconcentration reduce,the temperature enhances in the flow region.

Figs.11a displays the effect of nanoparticle volume fraction ϕ on the nanofluid velocity. It is found that as the nanoparticle volume fraction increases the nanofluid velocity in SWCNT'-Water nanofluid. These figures illustrate this agreement with the physical behaviour. When the volume of the nanoparticle increases the thermal conductivity and hence increases the momentum boundary layer thickness.Fig.11b shows that the variation of temperature with ϕ. It can be seen from the profiles that an increase in the nanoparticle volume fraction increases the temperature in the boundary layer. This is due to the fact that the thickness of the thermal boundary layer increases with increase in ϕ. Fig.11c shows the variation of concentration with nanoparticle volume fraction ϕ.We notice an enhancement in the concentration with increasing ϕ. This may be attributed to the fact that an enhancement in ϕ results in growth of the thickness of the solutal boundary layer.

The Skin friction(τ) ,Nusselt number(Nu) and Sherwood number(Sh) is exhibited in table.3 at the inner and outer cylinders for different parameters M, Rd,A11,B11,Ec,Sc,Q1,γ,ϕ, Δ. The variation of τ with magnetic parameter M shows that higher the Lorentz force smaller the skin friction at r=1&2.Nu and Sh increase on r=1 and reduces on r=2 with rise in M in SWCNT's nanofluid. With respect to space dependent heat source parameter (A11) we find that the skin friction (τ) enhances in SWCNT-water nanofluid on r=1 &2 with increasing A11>0 and for A11<0,we notice a depreciation in τ on both the cylinders. Nu and Sh increases on r=1 with rise in A11>0 and for A11<0,Nu Sh reduce on r=1. On r=2.Nu reduces and Sh enhances with A11>0 and for A11<0.

An increase in strength of the heat generating source (B11>0) reduces τ and depreciates with B11<0 on both the cylinders in SWCNT's-water nanofluid. Nu reduces and Sh enhances on r=1 with B11>0 and for B11<0,Nu enhances and Sh reduces. On r=2. Nu enhances and Sh reduces with rise in strength of the heat generating and for absorbing source (B11<0), Nu reduce and Sh enhances .An increase in the nano particle volume fraction ϕ increases τ on both the cylinders. Nu and Sh reduces on r=1 and they enhances on r=2 with rise in ϕ in SWCNT's-water nanofluid. The variation of τ with radiation parameter Rd shows that higher the radiative heat flux larger the magnitude of the skin friction and Sherwood number on both the cylinders. Nu enhances on r=1 and Sh enhances on r=2. An increase in Schmidt number (Sc) reduces the skin friction on both the cylinders. Nu enhances on r=1 and reduces on r=2 with Sc. Also it leads to an increment in Sh on r=1 and reduction in Sh on r=2.The skin friction (τ) reduces with γ>0 and reduces with γ<0 on r=1&2.Nu enhances on r=1 and reduces on r=2 in both degenerating /generating chemical reaction cases. Sh enhances on r=1 and reduces on r=2 in the degenerating chemical reaction case while in generating case, Nu & Sh reduces on r=1 and enhances on r=2. With respect to Forchheimer parameter (Δ) the skin friction enhances on both the cylinders with increase in Δ. An increase in Δ reduces Nu and enhances Sh on r=1 while on r=2,Nu enhances and Sh reduces with Δ. An increase in radiation absorption parameter (Q1) enhances τ and Sh on r=1and reduces on r=2.reduces Nu non r=1&2 (table 4).

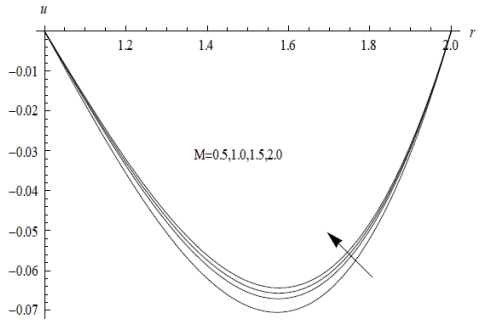

Fig.2a Variation of axial velocity(u) with M
Rd=0.5,Ec=0.01,Q1=0.5,Sc=0.66, A11=0.5, B11=0.5
γ=0.5,ϕ=0.1, Δ=0.2

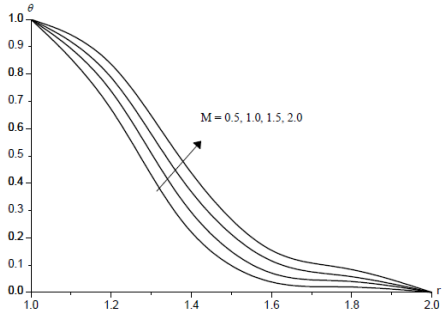

Fig.2b Variation of temperature(θ) with M
Rd=0.5,Ec=0.01,Q1=0.5,Sc=0.66, A11=0.5, B11=0.5
γ=0.5,ϕ=0.1, Δ=0.2

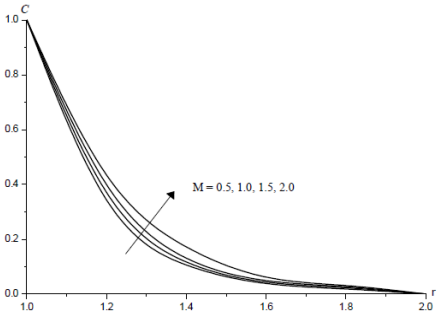

Fig.2c Variation of nanoconcentration(C) with M
Rd=0.5,Ec=0.01,Q1=0.5,Sc=0.66, A11=0.5, B11=0.5
γ=0.5,ϕ=0.1, Δ=0.2

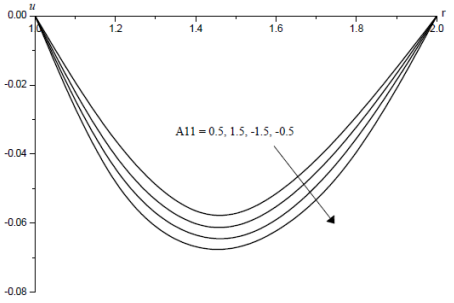

Fig.3a Variation of axial velocity(u) with A11
M=0.5, Rd=0.5,Ec=0.01,Q1=0.5,Sc=0.66, B11=0.5
γ=0.5,ϕ=0.1, Δ=0.2

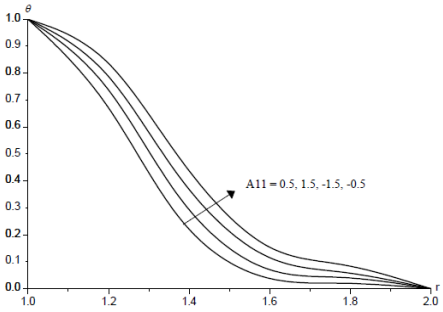

Fig.3b Variation of temperature(θ) with A11
M=0.5, Rd=0.5,Ec=0.01,Q1=0.5,Sc=0.66, B11=0.5
γ=0.5,ϕ=0.1, Δ=0.2

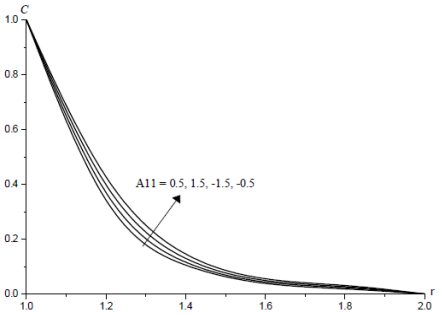

Fig.3c Variation of nanoconcentration(C) with A11
M=0.5, Rd=0.5,Ec=0.01,Q1=0.5,Sc=0.66, B11=0.5
γ=0.5,ϕ=0.1, Δ=0.2

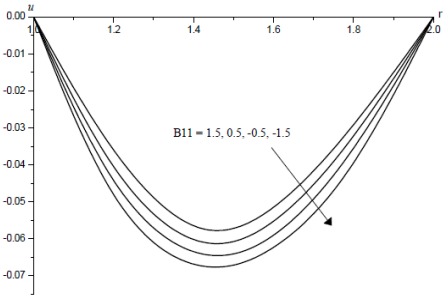

Fig.4a Variation of axial velocity(u) with B11
M=0.5, Rd=0.5,Ec=0.01,Q1=0.5,Sc=0.66, A11=0.5,
γ=0.5,ϕ=0.1, Δ=0.2

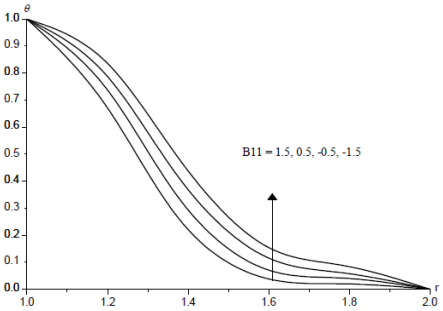

Fig.4b Variation of temperature(θ) with B11
M=0.5, Rd=0.5,Ec=0.01,Q1=0.5,Sc=0.66, A11=0.5,
γ=0.5,ϕ=0.1, Δ=0.2

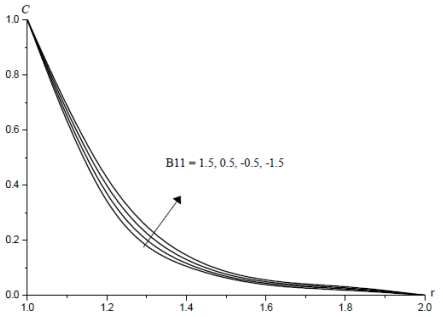

Fig.4c Variation of nanoconcentration(C) with B11
M=0.5, Rd=0.5,Ec=0.01,Q1=0.5,Sc=0.66, A11=0.5,
γ=0.5,ϕ=0.1, Δ=0.2

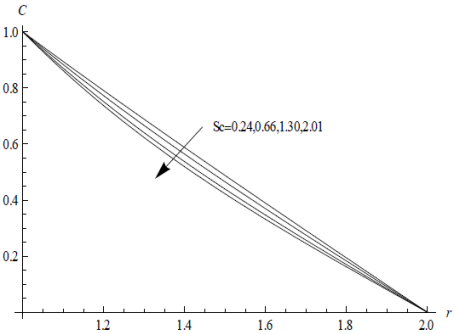

Fig.5c Variation of nanoconcentration(C) with Sc
M=0.5, Rd=0.5,Ec=0.01,Q1=0.5, A11=0.5, B11=0.5
γ=0.5,ϕ=0.1, Δ=0.2

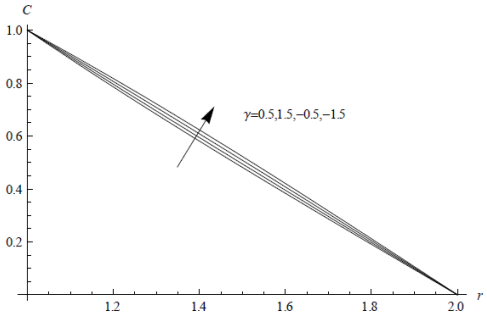

Fig.6c Variation of nanoconcentration(C) with γ
M=0.5, Rd=0.5,Ec=0.01,Q1=0.5,Sc=0.66, A11=0.5,
B11=0.5, ϕ=0.1, Δ=0.2

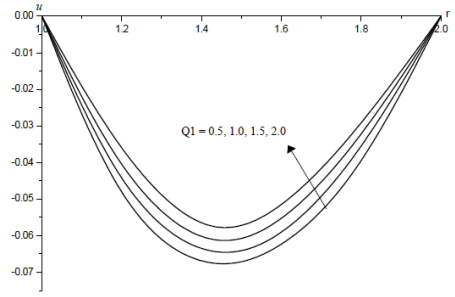

Fig.7a Variation of axial velocity(u) with Q1
M=0.5, Rd=0.5,Ec=0.01, Sc=0.66, A11=0.5,
B11=0.5, γ=0.5,ϕ=0.1, Δ=0.2

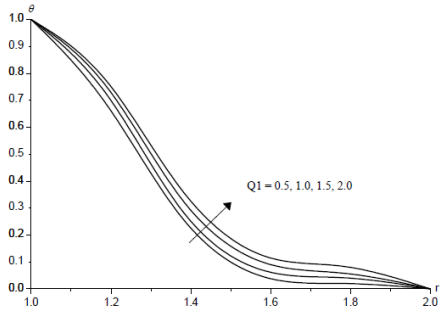

Fig.7b Variation of temperature(θ) with Q1
M=0.5, Rd=0.5,Ec=0.01, Sc=0.66, A11=0.5,
B11=0.5, γ=0.5,ϕ=0.1, Δ=0.2

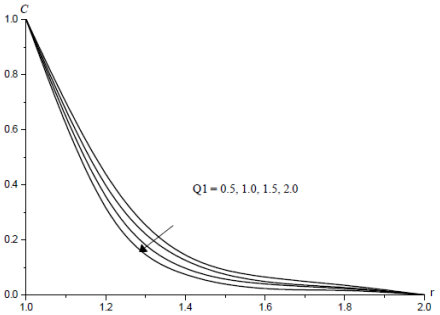

Fig.7c Variation of nanoconcentration(C) with Q1
M=0.5, Rd=0.5,Ec=0.01, Sc=0.66, A11=0.5,
B11=0.5, γ=0.5,ϕ=0.1, Δ=0.2

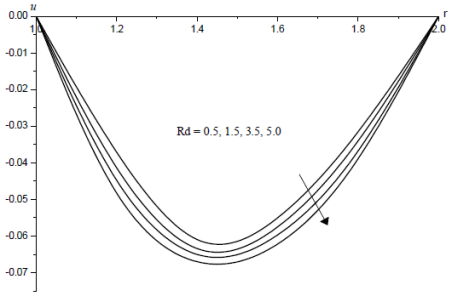

Fig.8a Variation of axial velocity(u) with Rd
M=0.5, Ec=0.01,Q1=0.5,Sc=0.66, A11=0.5,
B11=0.5, γ=0.5,ϕ=0.1, Δ=0.2

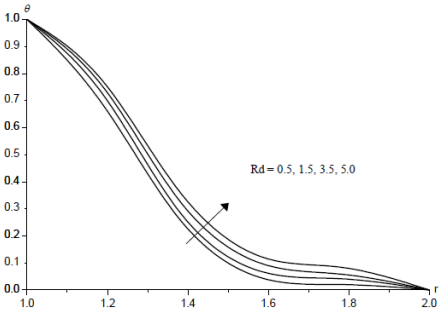

Fig.8b Variation of temperature(θ) with Rd
M=0.5, Ec=0.01,Q1=0.5,Sc=0.66, A11=0.5,
B11=0.5, γ=0.5,ϕ=0.1, Δ=0.2

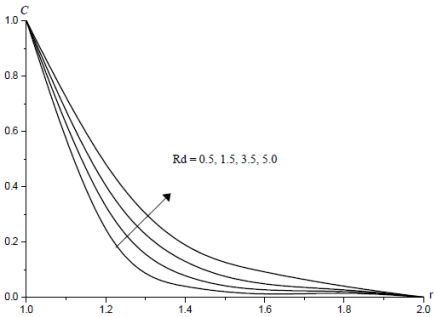

Fig.8c Variation of nanoconcentration(C) with Rd
M=0.5, Ec=0.01,Q1=0.5,Sc=0.66, A11=0.5,
B11=0.5, γ=0.5,ϕ=0.1, Δ=0.2

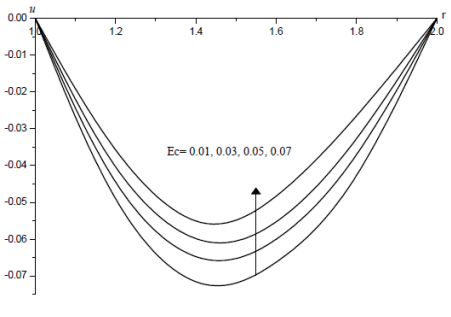

Fig.9a Variation of axial velocity(u) with Ec
M=0.5, Rd=0.5,Q1=0.5,Sc=0.66, A11=0.5, B11=0.5
γ=0.5,ϕ=0.1, Δ=0.2

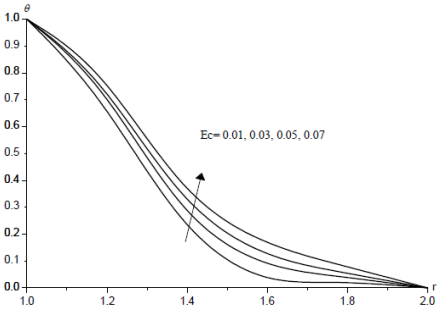

Fig.9b Variation of temperature(θ) with Ec
M=0.5, Rd=0.5, Q1=0.5,Sc=0.66, A11=0.5, B11=0.5
γ=0.5,ϕ=0.1, Δ=0.2

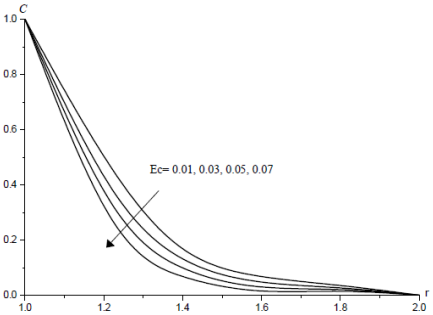

Fig.9c Variation of nanoconcentration(C) with Ec
M=0.5, Rd=0.5, Q1=0.5,Sc=0.66, A11=0.5, B11=0.5
γ=0.5,ϕ=0.1, Δ=0.2

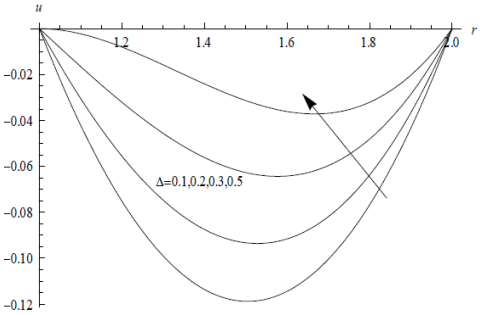

Fig.10a Variation of axial velocity(u) with Δ
M=0.5, Rd=0.5,Ec=0.01,Q1=0.5,Sc=0.66,
A11=0.5, B11=0.5, γ=0.5,ϕ=0.1

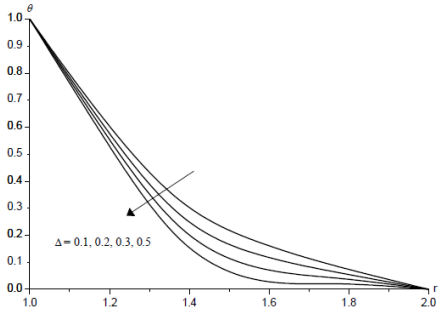

Fig.10b Variation of temperature(θ) with Δ
M=0.5, Rd=0.5,Ec=0.01,Q1=0.5,Sc=0.66,
A11=0.5, B11=0.5, γ=0.5,ϕ=0.1

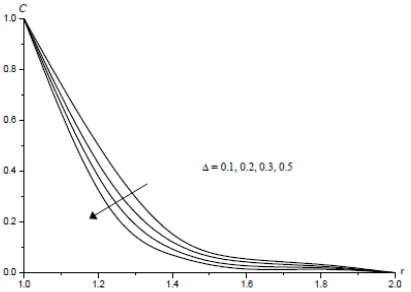

Fig.10c Variation of nanoconcentration(C) with Δ
M=0.5, Rd=0.5,Ec=0.01,Q1=0.5,Sc=0.66,
A11=0.5, B11=0.5, γ=0.5,ϕ=0.1

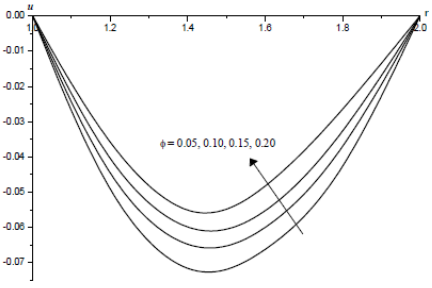

Fig.11a Variation of axial velocity(u) with ϕ
M=0.5, Rd=0.5,Ec=0.01,Q1=0.5,Sc=0.66,
A11=0.5, B11=0.5, γ=0.5, Δ=0.2

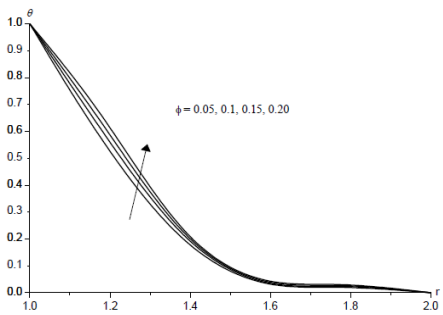

Fig.11b Variation of temperature(θ) with ϕ
M=0.5, Rd=0.5,Ec=0.01,Q1=0.5,Sc=0.66,
A11=0.5, B11=0.5, γ=0.5, Δ=0.2

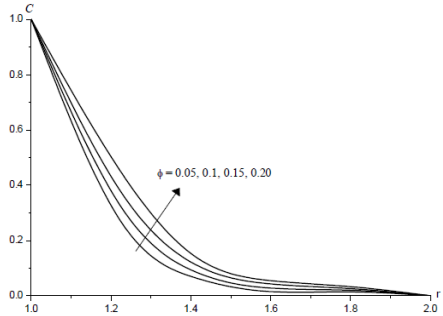

Fig.11c Variation of nanoconcentration(C) with ϕ
M=0.5, Rd=0.5,Ec=0.01,Q1=0.5,Sc=0.66,
A11=0.5, B11=0.5, γ=0.5, Δ=0.2

Table – 3 : Skin Friction (τ) and Nusslet number (Nu) at r = 1 & 2

Parameter		τ(1)	τ(2)	Nu(1)	Nu(2)	Parameter		τ(1)	τ(2)	Nu(1)	Nu(2)
M	0.5	-0.334342	0.417812	0.999954	1.00004	Φ	0.05	-0.167074	0.334017	0.999968	1.00006
	1	-0.168974	0.336185	0.999967	1.00003		0.1	-0.198163	0.34945	0.999966	1.00009
	1.5	-0.001793	0.253177	0.999976	1.00002		0.15	-0.244968	0.372769	0.999963	1.00013
	2	-0.001292	0.168124	0.999982	1.00001		0.2	-0.300647	0.400535	0.999958	1.00022
Rd	0.5	-0.167074	0.334017	0.999968	1.00005	Sc	0.24	-0.33434	0.417812	0.999954	1.00004
	1.5	-0.167076	0.334019	0.999993	1.00004		0.66	-0.167074	0.334017	0.999969	1.00003
	3.5	-0.167084	0.334021	0.999996	1.00003		1.3	-0.011751	0.250224	0.999978	1.00002
	5	-0.167165	0.334033	0.999997	1.00002		2.01	-0.007457	0.166431	0.999981	1.00001
Ec	0.01	-0.334342	0.417812	0.999954	1.00004	γ	0.5	-0.33434	0.417812	0.999954	1.00004
	0.03	-0.167074	0.334017	0.999965	1.00003		1.5	-0.167044	0.334017	0.999968	1.00003
	0.05	-0.011655	0.250223	0.999975	1.00002		-0.5	-0.010834	0.250223	0.999977	1.00002
	0.07	-0.010458	0.166429	0.999976	1.00001		-1.5	-0.019457	0.266643	0.99998	1.00001
A11	0.5	-0.167074	0.334017	0.999968	1.00003	Q1	0.5	-0.33434	0.417812	0.999954	1.00004
	1.5	-0.167076	0.334018	0.999972	1.00002		1.0	-0.167073	0.334016	0.999949	1.00003
	-0.5	-0.167074	0.334013	0.999967	1.00001		1.5	-0.104549	0.250221	0.999942	1.00002
	-1.5	-0.167073	0.333978	0.999964	1.00054		2.0	0.008462	0.166426	0.999938	1.00001
B11	0.5	-0.167074	0.334017	0.999968	1.00003	Δ	0.1	-0.33434	0.417812	0.999954	1.00004
	1.5	-0.167072	0.334014	0.999913	1.00006		0.2	3.26158	-1.41303	0.99903	1.00054
	-0.5	-0.167075	0.334018	0.999987	1.00002		0.3	10.6631	-5.32536	0.988735	1.00695
	-1.5	-0.167079	0.334022	1.000042	0.99999		0.5	12.8199	-12.1646	0.945462	1.03544

Table – 4 : Sherwood Number (Sh) at r = 1 & 2

Parameter		Sh(1)	Sh(2)	Parameter		Sh(1)	Sh(2)
M	0.5	1.06569	0.971147	Φ	0.05	1.06809	0.969049
	1	1.06805	0.969093		0.1	1.06765	0.969437
	1.5	1.07045	0.967006		0.15	1.06698	0.970022
	2	1.07291	0.964859		0.2	1.06618	0.970718
Rd	0.5	1.06809	0.969049	Sc	0.24	1.06569	0.971147
	1.5	1.06811	0.969054		0.66	1.19952	0.911469
	3.5	1.06819	0.969062		1.3	1.36818	0.836091
	5	1.06829	0.969071		2.01	1.65542	0.71333
Ec	0.01	1.06569	0.971147	γ	0.5	1.03046	0.988508
	0.03	1.06809	0.969048		1.5	1.10351	0.951794
	0.05	1.0705	0.966949		-0.5	0.960463	1.02172
	0.07	1.0729	0.964849		-1.5	0.888133	1.0578
A11	0.5	1.06809	0.969049	Q1	0.5	1.06569	0.971147
	1.5	1.06811	0.969055		1	1.0681	0.969047
	-0.5	1.06807	0.969047		1.5	1.0705	0.966947
	-1.5	1.06802	0.969043		2	1.07291	0.964846
B11	0.5	1.06809	0.969049	Δ	0.1	1.06569	0.971147
	1.5	1.06811	0.969043		0.2	1.11811	0.925286
	-0.5	1.06809	0.969051		0.3	1.23021	0.826879
	-1.5	1.06808	0.969057		0.5	1.42731	0.652845

7. CONCLUSIONS

The coupled equations governing the flow, heat and mass transfer have been solved by using Galerkin finite method with quadratic approximation functions. The velocity, temperature and concentration have been analysed for different parametric variations. The important conclusions of the analysis are

- Higher the Lorentz force smaller the velocity, larger the temperature and concentration in the flow region. The skin friction increases, the rate of heat and mass transfer increases on the inner cylinder and reduces on the outer cylinder with increase in M
- An increase in Rd enhances the velocity, temperat6ure and concentration in the flow region. The skin friction and Sherwood number enhances on both the cylinders. Nu enhances on r=1 and reduces on r=2 with Rd.
- With respect to Schmidt number Sc, we find that lesser the molecular diffusivity (Sc) smaller the concentration in the flow region. The skin friction reduce4s on r=1#&2.Nu and Sh enhances on r=1 and reduces on r=2 with increase in Sc.
- The velocity, concentration enhance, temperature reduces with increase in space dependent heat source (A11>0)while a reversed effect is noticed with A11<0. The velocity, concentration reduce, temperature enhances with increase in temperature dependent heat source(B11>0)while a reversed effect is noticed with B11<0..The skin friction τ, Sh enhances with A11>0 and reduces with A11<0 on both the cylinders. Nu enhances on r=1 and reduces on r=2 with A11>0 and reversed effect is noticed with A11<0 on the cylinders. An increase in B11>0, reduces the skin friction and enhances with B11<0.An increase in B11>0,reduces Nu on r=1 and Sh on r=2,Nu enhances on r=2,Sh reduces on r=1.An opposite be3haviour is noticed in them with 0<B11><0.
- Higher the dissipative energy smaller the velocity, concentration and larger the temperature in the flow region. The skin friction reduces on both the cylinders. On r=1,Nu and She enhances with Ec while they reduce on r=2.
- The velocity and concentration experience a depreciation, temperature enhances with increase in nano volume fraction (ϕ).The skin friction enhances, Nusselt and Sherwood numbers reduce on inner cylinder r=1 and enhance on r=2.with higher nano volume fraction.
- With reference to the chemical reaction parameter γ, we find that the concentration enhances in both the degenerating/generating chemical reaction cases. The skin friction reduces with $\gamma>0$ and reduces with $\gamma<0$ on both the cylinders. Nu enhances on r=1 and reduces on r=2 in both degenerating/generating chemical reaction cases. Sherwood number enhances on r=1 and reduces on r=2 in the degenerating chemical reaction case and in generating case, Sh reduces on inner cylinder and enhances on outer cylinder.
- An increase in radiation absorption parameter (Q1) reduces the velocity and concentration, enhances the temperature in the flow region. The skin friction and Sherwood number enhances on r=1 and reduces on r=2 with increase in Q1. Nu depreciates on r=1&2 with Q1.

8. REFERENCES

[1]. Abu-Nada, E., Masoud, Z., Hijazi, A: Natural convection heat transfer enhancement in horizontal concentric annuli using nanofluids, Int Commun Heat Mass Transf, V.35, 657-665(2008),

[2]. Abu-Nada, E: Effect of variable viscosity and thermal conductivity of Al_2O_3-water nanofluid on heat transfer enhancement in natural convection, Int J heat Fluid Flow, V.30, 679-690(2009).

[3]. Ahmad S., Tarawneh M., Yahya S. Y., and Rasid R., "Reinforced thermoplastic natural rubber (TPNR) composites with different types of carbon naotubes (MWNTS)," in *Carbon Nanotubes-Synthesis, Characterization, Applications*, S. Yellampalli, Ed., pp. 443–468, Open Access, London, UK, (2011).

[4]. Anuar N. S., Bachok N., Arifin N. M., and Rosali, H. "Role of multiple solutions in flow of nanofluids with carbon nanotubes over a vertical permeable moving plate," *Alexandria Engineering Journal*, vol. 59, no. 2, pp. 763–773, (2020).

[5]. Anuar N., Bachok N., and Pop I., "A stability analysis of solutions in boundary layer flow and heat transfer of carbon nanotubes over a moving plate with slip effect," *Energies*, vol. 11, no. 12, p. 3243, (2018).

[6]. Behzadmehr, A., Saffar-Avval, M., Galanis, N: Prediction of turbulent forced convection of a nanofluid in a tube with uniform heat flux using a two phase approach, Int J Heat Fluid Flow, V.28, 211-219(2007).

[7]. Berrehal H. and Maougal A., "Entropy generation analysis for multi-walled carbon nanotube (MWCNT) suspended nanofluid flow over wedge with thermal radiation and convective boundary condition," *Journal of Mechanical Science and Technology*, vol. 33, no. 1, pp. 459–464, (2019).

[8]. Bianco V., Chiacchio. F., Manca, O., Nardini, S: Numerical investigation of nanofluids forced convection in circular tubes, J. Appl Therm Eng, V.29, 3632-3642(2009).

[9]. Choi, S.U.S: Enhancing thermal conductivity of fluid with nanoparticles, developments and applications of non-Newtonian flow, ASME FED 231, 99-105(1995).

[10]. Cortell R. Fluid flow and radiative nonlinear heat transfer over a stretching sheet. J King Saud Univ Sci, 7,pp.26:161 (2014).

[11]. Das, S., Jana, R.N., and Makinde, O.D : Mixed convective magneto hydrodynamic flow in a vertical channel filled with nanofluids, Engineering science and technology an International Journal, V.18, 244-255(2015).

[12]. Ebaid S.A., Sharif, M : Application of Laplace transform for the exact effect of a magnetic field on heat transfer of carbon nanotubes suspended nanofluids, *Zeitschrift fur Naturforschung*, Vol.70, pp.471-475 (A 2015).

[13]. Emad M Abo-Eldahab and Mohamed A El Aziz: Blowing/Suction effect on hydromagnetic heat transfer by mixed convection from an inclined continuous stretching surface with internal heat generation/absorption., Int. J.Termal Sciences,V.43(7),pp.709-719(2004).

[14]. Hayat T, Qayyum S, Alsaedi A, Waqas M. Simultaneous influences of mixed convection and nonlinear thermal radiation in stagnation point flow of Oldroyd-B fluid towards an unsteady convectively heated stretched surface. J Mol Liq; 224:811–7 (2016).

[15]. Hong H, Wright B, Wensel J, Jin S, Ye XR, Roy W : Enhanced thermal conductivity by the magnetic field in heat transfer nanofluids containing carbon nanotube, Synth. Metals., Vol.157 (10–12), pp.437–440, (2007).

[16]. Jou, R.Y., Tzeng, S. C: Numerical research of nature convective heat transfer enhancement filled with nanofluids in rectangular enclosures, Int Commun Heat Mass Transf, V.33, 727-736(2006).

[17]. Kamali R, Binesh A : Numerical investigation of heat transfer enhancement using carbon nanotube-based non-Newtonian nanofluids, Int. Commun. Heat Mass Transf. Vol.37(8), pp.1153–1157, (2010)

[18]. Khan MI, Waqas M, Hayat T, Alsaedi A, Khan MI. Significance of nonlinear radiation in mixed convection flow of magneto Walter-B nanoliquid. Int J Hydrogen Energy (2017).

[19]. Khan W. A., Khan Z. H., and Rahi M., "Fluid flow and heat transfer of carbon nanotubes along a flat plate with Navier slip boundary," *Applied Nanoscience*, vol. 4, no. 5, pp. 633–641, (2014).

[20]. Kumaresan V, Velraj R, Das SK : Convective heat transfer characteristics of secondary refrigerant based CNT nanofluids in a tubular heat exchanger, Int. J. Refrig. Vol.35(8), pp. 2287–2296, (2012).

[21]. Lopez A, Ibanez G, Pantoja J, Moreira J, Lastres O. Entropy generation analysis of MHD nanofluid flow in a porous vertical microchannel with nonlinear thermal radiation, slip flow and convective-radiative boundary conditions. Int J Heat Mass Transf ;107:982–94, (2017).

[22]. Madhusudhana Reddy, Y., Rama Krishna, G.N. and Prasada Rao, D.R.V: Numerical study of Convective Flow of CuO-water and Al_2O_3-water nanofluids in cylindrical annulus, Int. Journal of Research & Development in Tech., Vol. 7, Issue 3, 142-148 (2017).

[23]. Maxwell J.C: Electricity and magnetism, Clarendon Press, Oxford, UK (1873).

[24]. Meyer J, McKrell T, Grote K : The influence of multi-walled carbon nanotubes on single-phase heat transfer and pressure drop characteristics in the transitional flow regime of smooth tubes, Int. J. Heat Mass Transf. Vol.58(1-2), pp.597–609, (2013).

[25]. Mokhtari Moghari, R., Akbarinia, A., Shariat, M., Talebi, F., Laur, R: Two phase mixed convection Al_2O_3-water nanofluid flow in an annulus, Int J Multiph Flow, V. 37(6), 585-595(2011).

[26]. Naganthran K., Nazar R., and Pop I., "Effects of heat generation/absorption in the Jeffery fluid past a permeable stretching/shrinking disc," *Journal of the Brazilian Society of Mechanical Sciences and Engineering*, vol. 41, pp. 1–12, (2019).

[27]. Oztop H. F. and Abu-Nada E., "Numerical study of natural convection in partially heated rectangular enclosures filled with nanofluids," *International Journal of Heat and Fluid Flow*, vol. 29, no. 5, pp. 1326–1336, (2008).

[28]. Pal D, Saha P. Influence of nonlinear thermal radiation and variable viscosity on hydromagnetic heat and mass transfer in a thin liquid film over an unsteady stretching surface. Int J Mech Sci 2016;119:208–16 (2016).

[29]. Pantokratoras A. Natural convection along a vertical isothermal plate with linear and nonlinear Rosseland thermal radiation. Int J Therm Sci ;84:151–7 (2014).

[29a] Park,B.C and Cho,Y.I:Hydrodynamic and heat transfer Heat transfer study of dispersed fluids with submicron metallic oxide particles,V.11,No.2,pp.151-170(1998)

[30]. Parvin, S., Nasrin, R., Alim, M.A., Hossain, N.F., Chamka, A. J: Thermal conductivity variation on natural convection flow of water-alumina nanofluid in an annulus, Int J Heat Mass Transf, V.55 (19-20), 5268-5274(2012).

[31]. Putra, N., Roetzel W, Das, S.K: Natural convection of nanofluids, Heat and Mass Transfer, V.39 (8-9), 775-784(2003).

[32]. Qayyum S, Khan MI, Hayat T, Alsaedi A. A framework for nonlinear thermal radiation and homogeneous-heterogeneous reactions flow based on silverwater and copper-water nanoparticles: A numerical model for probable error. Results Phys;7:1907–14 (2017).
[33]. Reddy JVR, Surunamma V, Sandeep N. Impact of nonlinear radiation on 3D magnetohydrodynamic flow of methanol and kerosene based ferrofluids with temperature dependent viscosity. J Mol Liquids; 236:39–100 (2017).
[34]. Santra, A.K., Sen, S., Chakraborty., N: Study of heat transfer due to laminar flow of copper-water nanofluid through two iso-thermally heated parallel plates, Int J Therm Sci., V.48, 391-400(2009).
[35]. Shafiq A., Khan I., Rasool G., Sherif E. M., and Sheikh A. H., "Influence of single- and multi-wall carbon nanotubes on magnetohydrodynamic stagnation point nanofluid flow over variable thicker surface with concave and convex effects," *Mathematics*, vol. 8, no. 104, (2020).
[36]. Sheikholeslami M, Ganji DD, Javed MY, Ellahi R. Effect of thermal radiation on magnetohydrodynamics nanofluid flow and heat transfer by means of two phase model. J Magn Magn Mater; 374:36–43 (2015).
[37]. Soleimani, S.I., Sheikholeslami, M., Ganji, D.D., Gorji-Bandpay, M: Natural convection heat transfer in a nanofluid filled semi annulus enclosure, Int Commun Heat Mass Transf, V.39 (4), 565-574(2012).
[38]. Sree Devi, G., Raghavendra Rao, R., Chamka, A.J and Prasada Rao, D.R.V: Mixed convective heat and mass transfer flow of nanofluids in concentric annulus with constant heat flux, Procedia Engineering, 127, 1048-1055(2015).
[39]. Sudarsana Reddy, P., Chamka, A.J: Soret and Dufour effects on MHD convective flow of Al2O3-water and TiO2- water nanofluids past a stretching sheet in porous media with heat generation/absorption, J. Advanced Powder Technology, V. 27, 1207-1218(2016).
[40]. Suochana G and Ramakrishna G N : Effect of Heat Sources on Non-Darcy Convective Heat and Mass Transfer Flow of Nanofluids in Cylindrical Annulus, *International Journal of Mathematical Archive (IJMA)*, Issue 6, Vol. 8, pp. 53-62 (2017), ISSN 2229-5046.
[41]. Tao, L.N: On combined and forced convection in channels, ASME J. Heat Transfer, V.82, 233-238(1960).
[42]. Tiwari R. K. and Das M. K.: "Heat transfer augmentation in a two-sided lid-driven differentially heated square cavity utilizing nanofluids," *International Journal of Heat and Mass Transfer*, vol. 50, no. 9-10, pp. 2002–2018, (2007).
[43]. Wang J, Zhu J, Zhang X, Chen Y : Heat transfer and pressure drop of nanofluids containing carbon nanotubes in laminar flows, Exp. Therm. Fluid. Sci. Vol. 44, pp. 716–721, (2013).
[44]. Wen, D and Ding, Y: Formulation of nanofluids for natural convective heat transfer applications, Int J Heat Fluid Flow, V. 26(6), 855-864(2005).
[45]. Xue QZ. Model for thermal conductivity of carbon nanotube-based composites. Phys B Condens Matter,–7, pp.368:302, (2005).